

Assemblies of Copper Bis(triazole) Coordination Polymers Using the Same Keggin Polyoxometalate Template

Ai-xiang Tian, Jun Ying, Jun Peng,* Jing-quan Sha, Hai-jun Pang, Peng-peng Zhang, Yuan Chen, Min Zhu, and Zhong-min Su*

Key Laboratory of Polyoxometalate Science of Ministry of Education, Faculty of Chemistry, Northeast Normal University, Changchun, Jilin 130024, People's Republic of China

Received July 17, 2008

Four inorganic–organic hybrid compounds, $[\text{Cu}^{\text{I}}_4(\text{bte})_4(\text{SiW}_{12}\text{O}_{40})]$ (**1**), $[\text{Cu}^{\text{II}}_2(\text{bte})_4(\text{SiW}_{12}\text{O}_{40})] \cdot 4\text{H}_2\text{O}$ (**2**) [bte = 1,2-bis(1,2,4-triazol-1-yl)ethane], $[\text{Cu}^{\text{I}}_4(\text{btb})_2(\text{SiW}_{12}\text{O}_{40})] \cdot 2\text{H}_2\text{O}$ (**3**), and $[\text{Cu}^{\text{II}}_2(\text{btb})_4(\text{SiW}_{12}\text{O}_{40})] \cdot 2\text{H}_2\text{O}$ (**4**) [btb = 1,4-bis(1,2,4-triazol-1-yl)butane], were hydrothermally synthesized through use of the same Keggin polyoxometalate as the template and tuning the molar ratio of the bis(triazole) ligand to the Cu^{II} ion. The ratio of the bis(triazole) ligand to Cu^{II} has a crucial influence on the structures of this series. Single-crystal X-ray diffraction analyses indicate that compound **1** is constructed by tetranuclear ring-connecting chains and polymerized $[\text{Cu}(\text{bte})]^+$ chains, between which SiW_{12} anions are inserted to form a three-dimensional (3D) structure. Compound **2** shows a $(4^4 \cdot 6^2)$ two-dimensional grid sheet. The discrete SiW_{12} anions are sandwiched by the sheets, just like “hamburgers”. Compound **3** presents channel-like $[\text{Cu}_2(\text{btb})]^{2+}$ polymerized chains, which are further connected by SiW_{12} anions to construct a 3D framework. Compound **4** exhibits a (6^6) 3D Cu-btb framework with hexagonal channels, into which the tetradentate SiW_{12} anions are incorporated. The thermal stabilities of the compounds are discussed.

Introduction

Polyoxometalates (POMs), as a unique class of inorganic metal oxide clusters, have received much attention not only because of their abundant structural diversity but also because of their versatile physical and chemical properties, such as catalytic activity, ion exchange, reversible redox behavior,

and photochromic or electrochromic response.^{1–3} Parallel to the rapid progress of POMs, a particular effort has been devoted to the family of transition-metal complexes (TMCs)-modified POMs, which brews an appealing route to design novel structures with improved properties.⁴

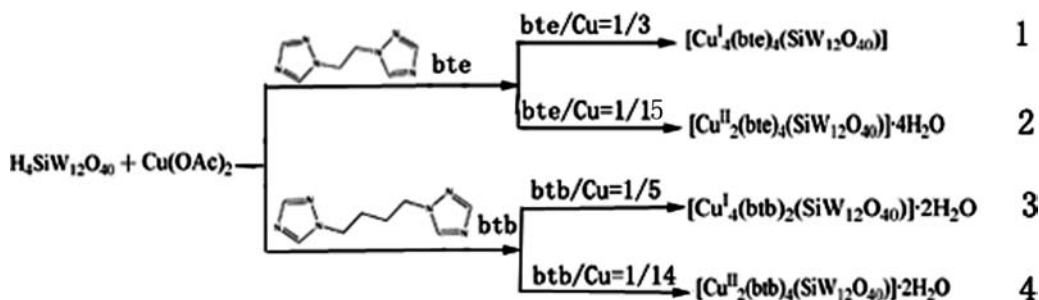
Compared with the template role of organic amines in zeolites and zeolite-like compounds,⁵ POMs acting as inorganic templates are explored not so long, whereas their merits are emerging: their versatile structural topologies and abundant chemical combinations endow them with controllable shape, size, and high negative charges. For example, Keller and co-workers used Keggin anions as templates to

* To whom correspondence should be addressed. E-mail: jpeng@nenu.edu.cn (J.P.), zmsu@nenu.edu.cn (Z.-m.S.). Tel.: +86 43185099667. Fax: +86 43185098768.

- (1) (a) Kamata, K.; Yamaguchi, S.; Kotani, M.; Yamaguchi, K.; Mizuno, N. *Angew. Chem., Int. Ed.* **2008**, *47*, 2407. (b) Sartorel, A.; Carraro, M.; Scorrano, G.; Zorzi, R.; Geremia, S.; McDaniel, N. D.; Bernhard, S.; Bonchio, M. *J. Am. Chem. Soc.* **2008**, *130*, 5006. (c) Macht, J.; Janik, M. J.; Necurock, M.; Iglesia, E. *Angew. Chem., Int. Ed.* **2007**, *46*, 7864. (d) Chen, L.-F.; Zhu, K.; Bi, L.-H.; Suchopar, A.; Reicke, M.; Mathys, G.; Jaensch, H.; Kortz, U.; Richards, R. M. *Inorg. Chem.* **2007**, *46*, 8457.
- (2) (a) Nyman, M.; Powers, C. R.; Bonhomme, F.; Alam, T. M.; Maginn, E. J.; Hobbs, D. T. *Chem. Mater.* **2008**, *20*, 2513. (b) Fernández, J. A.; López, X.; Bo, C.; Graaf, C.; Baerends, E. J.; Poblet, J. M. *J. Am. Chem. Soc.* **2007**, *129*, 12244. (c) Douvas, A. M.; Makarona, E.; Glezos, N.; Argitis, P.; Mielczarski, J. A.; Mielczarski, E. *ACS Nano* **2008**, *2*, 733.
- (3) (a) Mishra, P. P.; Pigga, J.; Liu, T.-B. *J. Am. Chem. Soc.* **2008**, *130*, 1548. (b) Schemberg, J.; Schneider, K.; Demmer, U.; Warkentin, E.; Müller, A.; Ermler, U. *Angew. Chem., Int. Ed.* **2007**, *46*, 2408. (c) Zhang, Y.-J.; Shen, Y.-F.; Yuan, J.-H.; Han, D.-X.; Wang, Z.-J.; Zhang, Q.-X.; Niu, L. *Angew. Chem., Int. Ed.* **2006**, *45*, 5867.

- (4) (a) Streb, C.; Ritchie, C.; Long, D.-L.; Kögerler, P.; Cronin, L. *Angew. Chem., Int. Ed.* **2007**, *46*, 7579. (b) Zheng, S.-T.; Zhang, J.; Yang, G.-Y. *Angew. Chem., Int. Ed.* **2008**, *47*, 3909. (c) Yokoyama, A.; Kojima, T.; Ohkubo, K.; Fukuzumi, S. *Chem. Commun.* **2007**, 3997. (d) Pichon, C.; Dolbecq, A.; Mialane, P.; Marrot, J.; Rivière, E.; Goral, M.; Zynek, M.; McCormac, T.; Borshch, S. A.; Zueva, E.; Sécheresse, F. *Chem.—Eur. J.* **2008**, *14*, 3189. (e) An, H.-Y.; Wang, E.-B.; Xiao, D.-R.; Li, Y.-G.; Su, Z.-M.; Xu, L. *Angew. Chem., Int. Ed.* **2006**, *45*, 904. (f) Botar, B.; Kögerler, P.; Hill, C. L. *Inorg. Chem.* **2007**, *46*, 5398. (g) Shivaiah, V.; Nagaraju, M.; Das, S. K. *Inorg. Chem.* **2003**, *42*, 6604.
- (5) (a) Yuan, H.-M.; Chen, J.-S.; Zhu, G.-S.; Li, J.-Y.; Yu, J.-H.; Yang, G.-D.; Xu, R.-R. *Inorg. Chem.* **2000**, *39*, 1476. (b) Zhang, M.; Zhou, D.; Li, J.-Y.; Yu, J.-H.; Xu, J.; Deng, F.; Li, G.-H.; Xu, R.-R. *Inorg. Chem.* **2007**, *46*, 136.

Scheme 1. Preparation Routes for Compounds 1–4



construct three Cu^{I} coordination polymers.⁶ Lu's group reported a series of Keggin POM-templated silver 1,2,4-triazole coordination polymers.⁷ Wang's group has hydrothermally synthesized a new double-Keggin-ion-templated, molybdenum-oxide-based inorganic–organic hybrid compound.⁸ However, most of the reports were based on rigid organic ligands to construct POM-templated frameworks and seldom based on flexible organic ligands such as 1,3-bis(4-pyridyl)propane.⁹ In this field, flexible ligands have more advantages than the rigid ones in that their flexibility and conformational freedom allow them to conform to the coordination environments of the transition-metal ions and POMs, which facilely exert the template role of POMs.¹⁰

Up to now, hydrothermal synthesis has become an important and successful technique for the preparation of TMCs-modified POM-based inorganic–organic hybrid compounds.¹¹ Unfortunately, from the crystal engineering point of view for targeting syntheses, hydrothermal reactions are commonly termed as “black box”, which can be affected by many factors such as the nature and stoichiometry of reactants, pH value, crystallization temperature, and reaction time.¹² However, to rationalize the reactivity pattern in the formation of targeting compounds under hydrothermal conditions, chemists have been systematically analyzing the chemistry involved in controlling reactions and, hence, the structures.^{13,14} For example, Long and co-workers have studied one after the other the effects of pH values, POM anions, and steric hindrance of organic ligands on the POM-based inorganic–organic hybrid compounds.^{15–17} Zubieta's group has discussed the influences of ligands and metal ions on the structures of molybdenum oxide networks.^{18,19} Frequently, the presence of some organic amines can reduce transition-metal ions under hydrothermal conditions.^{12b,20} However, the study on the reduction reactivity of organic amines is rare. In our previous work, we focused our investigation on the tuning of the spacer length of the bis(triazole) ligands to construct a series of POM-based compounds.^{10b} In this work, we give a special study of the quantitative effect of organic amines in the copper bis(triazole) system containing the same Keggin anion $[\text{SiW}_{12}\text{O}_{40}]^{4-}$ as the template, with the hope of obtaining informative examples for designable syntheses.

We have reported a series of $[\text{As}_8\text{V}_{14}\text{O}_{42}]^{4-}$ - and $[\text{V}_{16}\text{O}_{38}\text{Cl}]^{6-}$ -templated compounds using a flexible bis(imidazole) ligand.^{10a} For improving our synthetic strategy, in this work, we use the bis(triazole) ligand, which can unite the coordination geometry of both imidazole and pyrazole and provide

more potential coordination sites,²¹ to construct POM-templated compounds. Herein, we report four new inorganic–organic hybrid compounds, $[\text{Cu}^{\text{I}}_4(\text{bte})_4(\text{SiW}_{12}\text{O}_{40})]$ (**1**), $[\text{Cu}^{\text{II}}_2(\text{bte})_4(\text{SiW}_{12}\text{O}_{40})] \cdot 4\text{H}_2\text{O}$ (**2**) [bte = 1,2-bis(1,2,4-triazol-1-yl)ethane], $[\text{Cu}^{\text{I}}_4(\text{btb})_2(\text{SiW}_{12}\text{O}_{40})] \cdot 2\text{H}_2\text{O}$ (**3**), and $[\text{Cu}^{\text{II}}_2(\text{btb})_4(\text{SiW}_{12}\text{O}_{40})] \cdot 2\text{H}_2\text{O}$ (**4**) [btb = 1,4-bis(1,2,4-triazol-1-yl)butane] (Scheme 1). The influence of the molar ratio of organic amines to transition-metal ions on the structural assembly is discussed.

Experimental Section

Materials and General Methods. All reagents for syntheses were purchased from commercial sources and were used as received. Elemental analyses (C, H, and N) were performed on a Perkin-Elmer 2400 CHN elemental analyzer. The IR spectra were obtained on an Alpha Centaur FT-IR spectrometer with KBr pellet in the 400–4000 cm^{-1} region. X-ray photoelectron spectroscopy

- (6) (a) Inman, C.; Knaust, J. M.; Keller, S. W. *Chem. Commun.* **2002**, 156. (b) Knaust, J. M.; Inman, C.; Keller, S. W. *Chem. Commun.* **2004**, 492.
- (7) (a) Zhai, Q.-G.; Wu, X.-Y.; Chen, S.-M.; Zhao, Z.-G.; Lu, C.-Z. *Inorg. Chem.* **2007**, *46*, 5046. (b) Zhai, Q.-G.; Wu, X.-Y.; Chen, S.-M.; Chen, L.-J.; Lu, C.-Z. *Inorg. Chim. Acta* **2007**, *360*, 3484.
- (8) Li, Y.-G.; Dai, L.-M.; Wang, Y.-H.; Wang, X.-L.; Wang, E.-B.; Su, Z.-M.; Xu, L. *Chem. Commun.* **2007**, 2593.
- (9) Wang, X.-L.; Bi, Y.-F.; Chen, B.-K.; Lin, H.-Y.; Liu, G.-C. *Inorg. Chem.* **2008**, *47*, 2442.
- (10) (a) Dong, B.-X.; Peng, J.; Gómez-García, C. L.; Benmansour, S.; Jia, H.-Q.; Hu, N.-H. *Inorg. Chem.* **2007**, *46*, 5933. (b) Tian, A.-X.; Ying, J.; Peng, J.; Sha, J.-Q.; Han, Z.-G.; Ma, J.-F.; Su, Z.-M.; Hu, N.-H.; Jia, H.-Q. *Inorg. Chem.* **2008**, *47*, 3274.
- (11) Feng, S.-H.; Xu, R.-R. *Acc. Chem. Res.* **2001**, *34*, 239.
- (12) (a) Pavani, K.; Ramanan, A. *Eur. J. Inorg. Chem.* **2005**, 3080. (b) Pavani, K.; Lofland, S. E.; Ramanujachary, K. V.; Ramanan, A. *Eur. J. Inorg. Chem.* **2007**, 568.
- (13) Zhao, J.-W.; Zhang, J.; Zheng, S.-T.; Yang, G.-Y. *Chem. Commun.* **2008**, 570.
- (14) (a) Sha, J.-Q.; Peng, J.; Tian, A.-X.; Liu, H.-S.; Chen, J.; Zhang, P.-P.; Su, Z.-M. *Cryst. Growth. Des.* **2007**, *7*, 2535. (b) Sha, J.-Q.; Peng, J.; Liu, H.-S.; Chen, J.; Tian, A.-X.; Zhang, P.-P. *Inorg. Chem.* **2007**, *46*, 11183.
- (15) Zheng, P.-Q.; Ren, Y.-P.; Long, L.-S.; Huang, R.-B.; Zheng, L.-S. *Inorg. Chem.* **2005**, *44*, 1190.
- (16) Ren, Y.-P.; Kong, X.-J.; Long, L.-S.; Huang, R.-B.; Zheng, L.-S. *Cryst. Growth. Des.* **2006**, *6*, 572.
- (17) Ren, Y.-P.; Kong, X.-J.; Hu, X.-Y.; Sun, M.; Long, L.-S.; Huang, R.-B.; Zheng, L.-S. *Inorg. Chem.* **2006**, *45*, 4016.
- (18) Hagrman, P. J.; LaDuca, R. L.; Koo, H. J.; Rarig, R.; Haushalter, R. C.; Whangbo, M. H.; Zubieta, J. *Inorg. Chem.* **2000**, *39*, 4311.
- (19) Hagrman, P. J.; Zubieta, J. *Inorg. Chem.* **2000**, *39*, 5218.
- (20) (a) Zhang, X.-M.; Tong, M.-L.; Chen, X.-M. *Angew. Chem., Int. Ed.* **2002**, *41*, 1029. (b) Liu, C.-M.; Zhang, D.-Q.; Zhu, D.-B. *Cryst. Growth Des.* **2005**, *5*, 1639. (c) Wang, X.-L.; Qin, C.; Wang, E.-B.; Su, Z.-M. *Chem. Commun.* **2007**, 4245.
- (21) (a) Beckmann, U.; Brooker, S. *Coord. Chem. Rev.* **2003**, *245*, 17. (b) Haasnoot, J. G. *Coord. Chem. Rev.* **2000**, *200–202*, 131. (c) Wang, X.-L.; Qin, C.; Wang, E.-B.; Su, Z.-M.; Li, Y.-G.; Xu, L. *Angew. Chem., Int. Ed.* **2006**, *45*, 7411.

Table 1. Crystal Data and Structure Refinements for Compounds **1–4**

	1	2	3	4
formula	C ₂₄ H ₃₂ Cu ₄ N ₂₄ O ₄₀	C ₂₄ H ₄₀ Cu ₂ N ₂₄ O ₄₄	C ₁₆ H ₂₈ Cu ₄ N ₁₂ O ₄₂	C ₃₂ H ₅₂ Cu ₂ N ₂₄ O ₄₂
fw	SiW ₁₂ 3785	SiW ₁₂ 3730	SiW ₁₂ 3548.8	3806.15
cryst syst	monoclinic	monoclinic	triclinic	monoclinic
space group	<i>P</i> 2 ₁ / <i>n</i>	<i>P</i> 2 ₁ / <i>n</i>	<i>P</i> $\bar{1}$	<i>P</i> 2 ₁ / <i>n</i>
<i>a</i> (Å)	14.5861(5)	13.460(3)	11.4870(11)	11.2015(6)
<i>b</i> (Å)	27.3532(9)	16.745(3)	11.5977(11)	14.9693(8)
<i>c</i> (Å)	16.4118(5)	15.169(3)	11.6541(11)	21.4585(11)
α (deg)			98.9080(10)	
β (deg)	90.35	109.66(3)	107.6000(10)	92.0980(10)
γ (deg)			109.7280(10)	
<i>V</i> (Å ³)	6547.8(4)	3219.6(11)	1334.7(2)	3595.7(3)
<i>Z</i>	4	2	1	2
<i>D</i> _c (g cm ⁻³)	3.840	3.839	4.410	3.512
μ (mm ⁻¹)	22.377	22.119	27.424	19.807
<i>F</i> (000)	6728	3312	1558	3408
final <i>R</i> ¹ ^a , <i>wR</i> ² ^b [<i>I</i> > 2 σ (<i>I</i>)]	0.0713, 0.1672	0.0692, 0.1507	0.0896, 0.2406	0.0606, 0.1594
final <i>R</i> ¹ ^a , <i>wR</i> ² ^b (all data)	0.0884, 0.1776	0.0872, 0.1604	0.0929, 0.2426	0.0750, 0.1664
GOF on <i>F</i> ²	1.057	1.053	1.105	1.085
largest diff peak and holes (e Å ⁻³)	14.274 and -7.879	5.024 and -6.901	4.352 and -2.829	2.147 and -3.254

$$^a R1 = \sum |F_o| - |F_c| / \sum |F_o|, \quad ^b wR2 = \{ \sum [w(F_o^2 - F_c^2)]^2 / \sum [w(F_o^2)]^2 \}^{1/2}$$

(XPS) analyses were performed on a VG ESCALAB MK II spectrometer with a Mg Ka (1253.6 eV) achromatic X-ray source. The vacuum inside the analysis chamber was maintained at 6.2×10^{-6} Pa during analysis. The thermogravimetric analyses (TGA) were carried out in N₂ on a Perkin-Elmer DTA 1700 differential thermal analyzer with a rate of 10.00 °C min⁻¹. Electrochemical measurements were performed with a CHI 660b electrochemical workstation. A conventional three-electrode system was used with Ag/AgCl (3 M KCl) as a reference electrode and Pt wire as a counter electrode. Chemically bulk-modified carbon-paste electrodes (CPEs) were used as the working electrodes.

Synthesis of [Cu^I₄(bte)₄(SiW₁₂O₄₀)] (1). A mixture of H₄[SiW₁₂O₄₀]·14H₂O (0.47 g, 0.15 mmol), Cu(CH₃COO)₂·2H₂O (0.675 g, 3.1 mmol), and bte (0.164 g, 1 mmol) was dissolved in 10 mL of distilled water at room temperature. When the pH value of the mixture was adjusted to about 4.2 with 1.0 mol L⁻¹ HCl, the suspension was put into a Teflon-lined autoclave and kept under autogenous pressure at 160 °C for 4 days. After slow cooling to room temperature, orange block crystals were filtered and washed with distilled water (30% yield based on W). Anal. Calcd for C₂₄H₃₂Cu₄N₂₄O₄₀SiW₁₂ (3785): C, 7.61; H, 0.85; N, 8.88. Found: C, 7.58; H, 0.87; N, 8.83. IR (solid KBr pellets, cm⁻¹): 3835 (w), 3739 (w), 3609 (w), 3126 (w), 1686 (w), 1617 (w), 1533 (s), 1427 (w), 1350 (w), 1278 (m), 1216 (w), 1141 (w), 974 (s), 921 (s), 871 (w), 790 (s).

Synthesis of [Cu^{II}₂(bte)₄(SiW₁₂O₄₀)]·4H₂O (2). Compound **2** was prepared similarly to compound **1**, except for a change in the weight of the bte ligand (0.033 g, 0.21 mmol). Dark-blue block crystals were filtered and washed with distilled water (30% yield based on W). Anal. Calcd for C₂₄H₄₀Cu₂N₂₄O₄₄SiW₁₂ (3730): C, 7.72; H, 1.07; N, 9.01. Found: C, 7.67; H, 1.1; N, 8.97. IR (solid KBr pellets, cm⁻¹): 3780 (w), 3662 (w), 3123 (w), 1677 (w), 1598 (w), 1529 (s), 1440 (m), 1364 (w), 1280 (s), 1213 (m), 1128 (s), 985 (s), 923 (s), 878 (w), 792 (s).

Synthesis of [Cu^I₄(btb)₂(SiW₁₂O₄₀)]·2H₂O (3). A mixture of H₄[SiW₁₂O₄₀]·14H₂O (0.47 g, 0.15 mmol), Cu(CH₃COO)₂·2H₂O (0.55 g, 2.5 mmol), and btb (0.082 g, 0.5 mmol) was dissolved in 10 mL of distilled water at room temperature. When the pH value of the mixture was adjusted to about 4.3 with 1.0 mol L⁻¹ HCl, the suspension was put into a Teflon-lined autoclave and kept under autogenous pressure at 160 °C for 4 days. After slow cooling to room temperature, dark-orange block crystals were filtered and washed with distilled water (30% yield based on W). Anal. Calcd

for C₁₆H₂₈Cu₄N₁₂O₄₂SiW₁₂ (3548.8): C, 5.41; H, 0.79; N, 4.73. Found: C, 5.37; H, 0.82; N, 4.68. IR (solid KBr pellets, cm⁻¹): 3855 (w), 3750 (w), 3671 (w), 3438 (m), 3123 (w), 1686 (w), 1644 (w), 1617 (w), 1538 (s), 1453 (w), 1364 (w), 1297 (m), 1206 (w), 1143 (m), 967 (m), 919 (s), 878 (w), 788 (s).

Synthesis of [Cu^{II}₂(btb)₄(SiW₁₂O₄₀)]·2H₂O (4). Compound **4** was prepared similarly to compound **3**, except for a change in the the weight of the btb ligand (0.034 g, 0.18 mmol). Blue block crystals were filtered and washed with distilled water (25% yield based on W). Anal. Calcd for C₃₂H₅₂Cu₂N₂₄O₄₂SiW₁₂ (3806.15): C, 10.1; H, 1.37; N, 8.83. Found: C, 10.05; H, 1.39; N, 8.78. IR (solid KBr pellets, cm⁻¹): 3842 (w), 3732 (w), 3623 (w), 3118 (w), 1678 (w), 1527 (s), 1453 (m), 1370 (w), 1280 (s), 1211 (w), 1132 (s), 979 (m), 923 (s), 871 (w), 796 (s).

Preparations of 1-, 2-, 3-, and 4-CPEs. The compound **1**-modified CPE (**1**-CPE) was fabricated as follows: 90 mg of graphite powder and 8 mg of **1** were mixed and ground together by an agate mortar and pestle to achieve a uniform mixture, and then 0.1 mL of Nujol was added with stirring. The homogenized mixture was packed into a glass tube with a 1.5 mm inner diameter, and the tube surface was wiped with paper. Electrical contact was established with a Cu rod through the back of the electrode. In a similar manner, **2**-, **3**-, and **4**-CPEs were made with compounds **2–4**.

X-ray Crystallographic Study. X-ray diffraction analysis data for compounds **1–4** were collected with a Bruker Smart Apex CCD diffractometer with Mo K α ($\lambda = 0.71073$ Å) at 293 K. The structures were solved by direct methods and refined on *F*² by full-matrix least-squares methods using the *SHELXTL* package.²² For the compounds, all of the H atoms attached to C atoms were generated geometrically, while the H atoms attached to water molecules were not located but were included in the structure factor calculations. A summary of their crystallographic data and structural determination is provided in Table 1. Selected bond lengths and angles of the four compounds are listed in Table S1 (Supporting Information). Crystallographic data for the structures reported in this paper have been deposited in the Cambridge Crystallographic Data Centre as CCDC 691699 for **1**, 691700 for **2**, 691701 for **3**, and 691702 for **4**. The coordinates can be obtained, upon request,

(22) (a) Sheldrick, G. M. *SHELXS-97, Program for Crystal Structure Solution*; University of Göttingen: Göttingen, Germany, 1997. Sheldrick, G. M. *SHELXL-97, Program for Crystal Structure Refinement*; University of Göttingen: Göttingen, Germany, 1997.

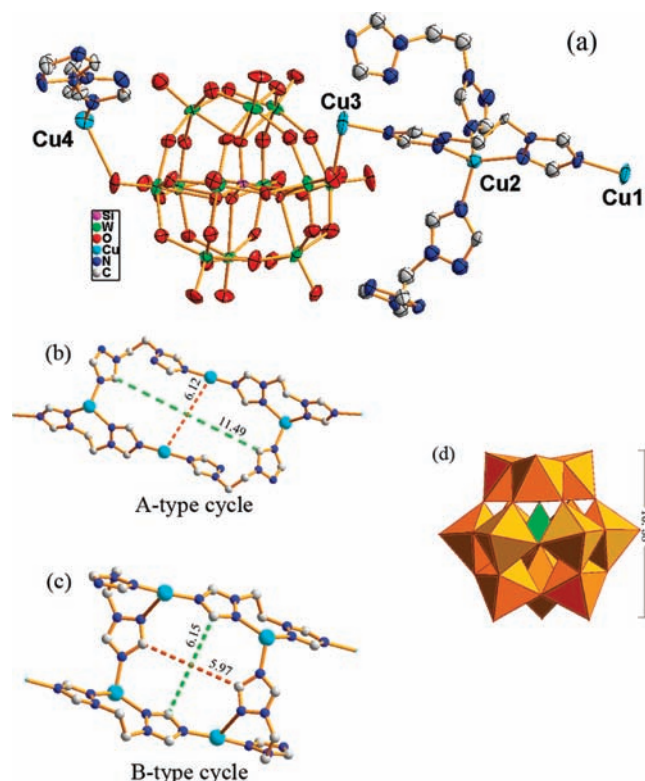


Figure 1. (a) ORTEP drawing of **1** with thermal ellipsoids at 50% probability. The H atoms have been omitted for clarity. (b and c) A- and B-type tetranuclear cycles with different dimensions in **1**. Color code: blue ball, Cu^I ion. (d) Polyhedral representation of the Keggin-type SiW₁₂ anion. Color code: green polyhedron, SiO₄; orange polyhedron, WO₆.

from the Director, Cambridge Crystallographic Data Centre, 12 Union Road, Cambridge CB2 1EZ, U.K.

Results and Discussion

The [SiW₁₂O₄₀]⁴⁻ (abbreviated to SiW₁₂) anion is the inorganic building block in compounds **1–4**. However, in compounds **2–4**, the central four μ_4 -O atoms are observed to be disordered over eight positions with each oxygen site half-occupied, a usual problem for POM clusters.²³ Bond valence sum calculations²⁴ show that all W atoms are in the VI+ oxidation state and Cu atoms are in the I+ oxidation state in compounds **1** and **3** and the II+ oxidation state in **2** and **4**. The oxidation states of Cu atoms are further confirmed by XPS spectra.

Crystal Structure of Compound 1. Crystal structure analysis reveals that compound **1** consists of four Cu^I ions, four bte ligands, and one SiW₁₂ anion (Figure 1a).

In compound **1**, the Cu^I ion adopts the distorted T-type geometry, coordinated by three N atoms from two bte ligands, with Cu–N bond distances of 1.875(2)–2.591(2) Å and N–Cu–N angles of 82.4(6)–169.8(8)°. The Cu^{II} ion is four-coordinated in a “seesaw” geometry, coordinated by four N atoms from three bte ligands. The bond distances and angles around Cu^{II} ion are 1.995(19)–2.104(16) Å for

Cu–N and 104.6(7)–114.2(7)° for N–Cu–N. The Cu^{III} ion is also in a “seesaw” geometry, coordinated by three N atoms from three bte ligands and one O atom from the SiW₁₂ anion, with Cu–N bond distances of 1.864(2)–2.748(2) Å, N–Cu–N angles of 85.9(3)–169.1(8)°, and N–Cu–O angles of 78.7(9)–108.6(4)°. The Cu^{IV} ion adopts the T-type geometry, coordinated by two N atoms from two bte ligands and one O atom from the SiW₁₂ anion, with Cu–N bond distances of 1.854(2) and 1.863(2) Å, a Cu–O bond distance of 2.738(2) Å, a N–Cu–N angle of 172.5(8)°, and N–Cu–O angles of 87.07(2) and 98.5(4)°.

In compound **1**, the bte ligand, acting as both a bridging linker and a chelator, exhibits diverse coordination modes (Table 2): It acts as a bidentate linkage, bridging two Cu^I ions through two apical N atoms (a type); it acts as a tridentate linkage, providing two N atoms to chelate one Cu^I ion and one of the two remaining apical N atoms to bridge one Cu^I ion (b type); it acts as a tetradentate linkage, using two apical N atoms to bridge two Cu^I ions and two N atoms to chelate one Cu^I ion (c type); it utilizes three of the four N atoms to link three Cu^I ions, acting as a tridentate linkage in an unusual asymmetrical coordination mode (d type). Such diversity of the coordination modes of the bte ligand in metal coordination polymers is scarce.

Noticeably, there are two types of tetranuclear cycles in compound **1**. The first one (A type) uses two a-type and two c-type bte molecules to link four Cu^I ions and form a tetranuclear cycle with a dimension of ca. 11.49 × 6.12 Å (Figure 1b), while the second one (B type) uses two b-type and two c-type bte molecules to form a cycle with a dimension of ca. 6.15 × 5.97 Å (Figure 1c). Through further sharing of the c-type bte molecule (Figure S1 in the Supporting Information), the two types of tetranuclear cycles are perpendicularly linked and alternately arrayed to construct a chain of ring connecting ring (Figure 2a). The SiW₁₂ anions connect with the A-type cycles in an up-and-down mode without being enveloped perhaps as a result of its big volume (ca. 10.38 × 10.38 Å; Figure 1d). Besides the ring-connecting chain unit in **1**, there also exists a [Cu(bte)]⁺ chain unit, as shown in Figure 2b, right. The two types of chains perpendicularly connect together through sharing of the same Cu^{III} ions and SiW₁₂ anions alternately to generate the three-dimensional (3D) framework (Figure 2b, left). The covalent linkages between the chain layers stabilize the whole structure.

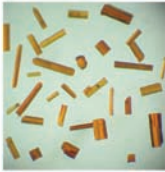
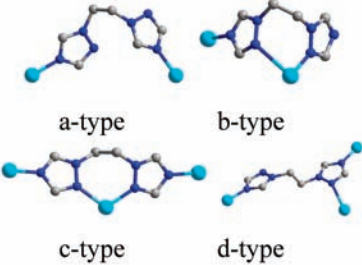


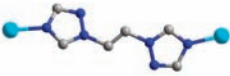

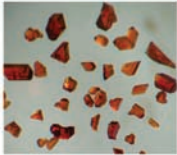
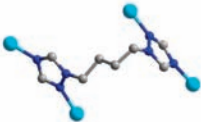
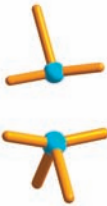

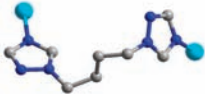

Crystal Structure of Compound 2. Crystal structure analysis reveals that compound **2** consists of two Cu^{II} ions, four bte ligands, one SiW₁₂ anion, and four water molecules (Figure 3a). In **2**, each Cu^{II} ion is five-coordinated by four N atoms of four bte ligands and one water molecule in a square-pyramidal geometry, having a τ value of 0.2 [$\tau = (\beta - \alpha)/60$],²⁵ with the angles N1–Cu1–N7 = 175.81° (β) and N6–Cu1–N12 = 163.56° (α). The bond distances around the Cu^{II} ions are 1.983(14)–2.03(15) Å (Cu–N) and 2.25(19) Å (Cu–O), which are similar to those in the five-

(23) (a) Evans, H. T.; Pope, M. T. *Inorg. Chem.* **1984**, *23*, 501. (b) Gao, G.-G.; Xu, L.; Wang, W.-J.; Qu, X.-S.; Liu, H.; Yang, Y.-Y. *Inorg. Chem.* **2008**, *47*, 2325. (c) Shi, Z.-Y.; Gu, X.-J.; Peng, J.; Yu, X.; Wang, E.-B. *Eur. J. Inorg. Chem.* **2006**, 385.

(24) Brown, I. D.; Altermatt, D. *Acta Crystallogr., Sect. B* **1985**, *41*, 244.

(25) Addison, A. W.; Rao, T. N. *J. Chem. Soc., Dalton Trans.* **1984**, 1349.

Table 2. Crystal Photographs, Coordination Numbers, and Modes of L (L = bte and btb) and Cu Ions in Compounds 1–4

	crystal photo	coordination number and mode of L	coordination number and mode of copper ions
1		 <p>a-type b-type c-type d-type</p>	
2			
3			
4			

coordinated Cu^{II} complexes.^{4e,10b,26} The bte molecule in compound **2** only acts as a bidentate bridging ligand using two apical N atoms (Table 2).

Each Cu^{II} ion links four bte molecules, while each bte molecule acts as a bidentate ligand to bridge two Cu^{II} ions. Thus, a grid sheet is formed with a Schläfli symbol of 4⁴·6². Owing to the single coordination mode for the Cu^{II} ion, as well as for the bte ligand, the grids are uniform with a dimension of 11.19 × 10.71 Å (Figure 3b).

These cationic sheets are paired and are parallel with each other, between which the SiW₁₂ anions are sandwiched to form a layer unit in compound **2**, as shown in Figure 4. The SiW₁₂ anions are not encircled, perhaps for the same reason as that in compound **1**. The adjacent layers are stagger-peaked, as shown in Figure 5. This kind of packing mode may decrease the molecular repulsion and stabilize the whole structure.

Crystal Structure of Compound 3. Crystal structure analysis reveals that compound **3** consists of four Cu^I ions, two btb ligands, one SiW₁₂ anion, and two water molecules (Figure 6a).

In compound **3**, there are two coordination geometries of Cu^I ions. The Cu1 ion is three-coordinated in a T-type geometry, coordinated by two N atoms from two btb ligands and one O atom of the SiW₁₂ anion. The bond distances and angles around Cu1 ion are 1.88(3) and 1.94(16) Å for Cu–N, 2.75(7) Å for Cu–O, 165(6)° for N–Cu–N, and 85.7(4) and 100.2(3)° for N–Cu–O. The Cu2 ion is four-coordinated in a “seesaw” geometry, coordinated by two N atoms from two btb ligands, one O atom of the SiW₁₂ anion, and one water molecule. The bond distances and angles around the Cu2 ion are 1.92(3) and 1.95(10) Å for Cu–N, 2.21(1) and 2.56(2) Å for Cu–O, 158(3)° for Cu–N, and 89.0(6)–101.0(9)° for N–Cu–O. The btb molecule utilizes all of the four N donors to link four Cu^I ions, acting as a tetradentate bridging ligand (Table 2).

There exist two kinds of dinuclear cycles in compound **3**: One is constructed by two btb ligands connected by two Cu^I

(26) (a) Cao, R.-G.; Liu, S.-X.; Xie, L.-H.; Pan, Y.-B.; Cao, J.-F.; Ren, Y.-H.; Xu, L. *Inorg. Chem.* **2007**, *46*, 3541. (b) Lisnard, L.; Dolbecq, A.; Mialane, P.; Marrot, J.; Cadjovi, E.; Sécheresse, F. *J. Chem. Soc., Dalton Trans.* **2005**, 3913.

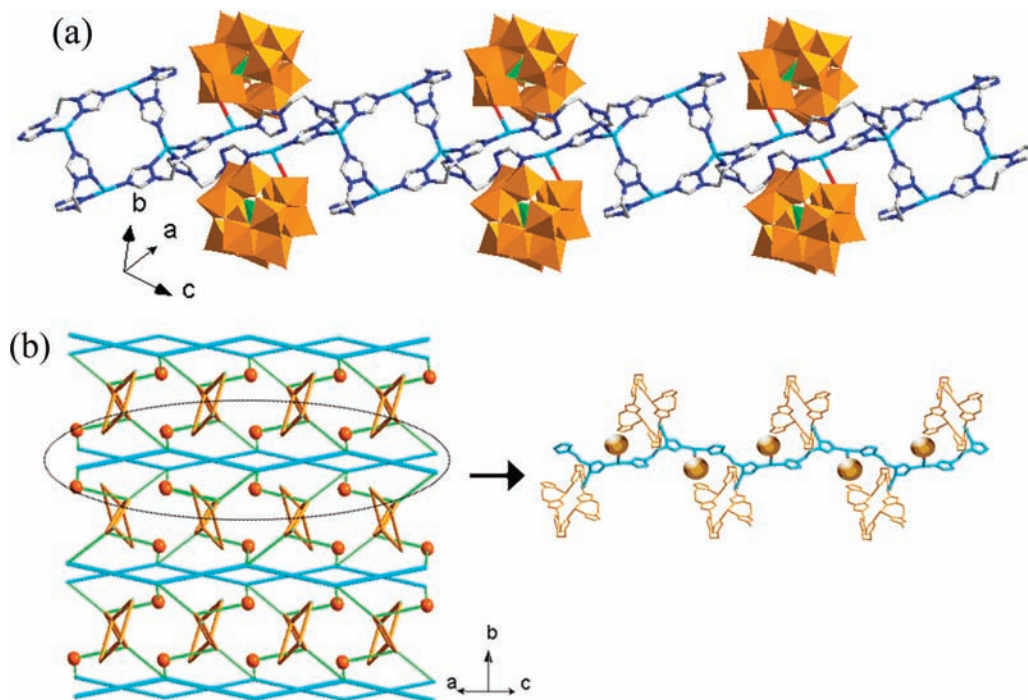


Figure 2. (a) Ring-connecting chain in **1** with the SiW_{12} anions suspended up and down of the A-type cycles. (b) Left: Ring-connecting chains (yellow) and SiW_{12} anions (orange balls) covalently linked by the $[\text{Cu}(\text{bte})]^+$ chains (blue) to construct a 3D framework. Right: Mode of the $[\text{Cu}(\text{bte})]^+$ chain (blue) connecting the ring-connecting chains (yellow) and SiW_{12} anions (yellow balls) alternately.

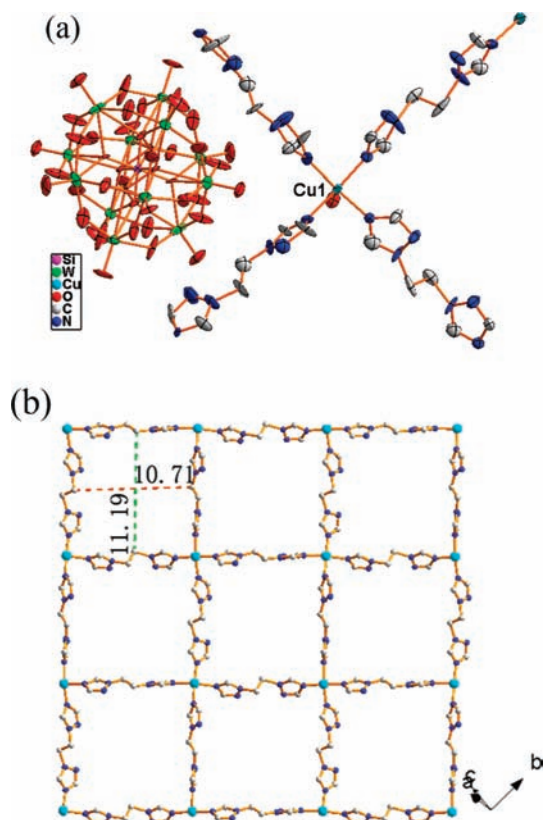


Figure 3. (a) ORTEP drawing of **2** with thermal ellipsoids at 50% probability. The water molecules and H atoms have been omitted for clarity. (b) Grid sheet in **2**.

ions with a dimension of ca. $7.97 \times 6.9 \text{ \AA}$. The other is connected by two Cu2 ions with a dimension of ca. $6.35 \times 4.42 \text{ \AA}$, as shown in Figure 6b. These two noncoplanar cycles with a dihedral angle of 122.7° connect with each other by

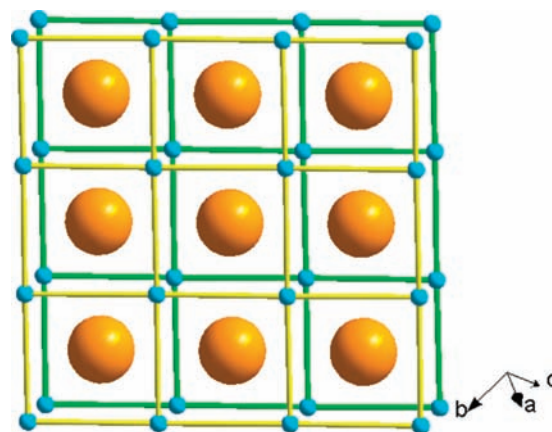


Figure 4. Two adjacent cationic sheets sandwiching the discrete anions (orange balls) in **2**.

sharing a btb ligand to form a corrugated loop that repeatedly arranges, forming a channel-like chain (Figure 7a). The SiW_{12} anions are sandwiched by the channel-like chains with covalent bonding onto the Cu1 ions via their two bridging O atoms, leading to a two-dimensional (2D) layer, as shown in Figure 7b. Moreover, each SiW_{12} anion also provides two terminal O atoms to link the Cu2 ions of the adjacent layers, and thus these layers are united to construct a 3D framework (Figure S2 in the Supporting Information).

Crystal Structure of Compound 4. Crystal structure analysis reveals that compound **4** consists of two Cu^{II} ions, four btb ligands, one SiW_{12} anion, and two water molecules (Figure 8a). Each Cu^{II} ion is six-coordinated in an octahedron geometry, coordinated by four N atoms from four btb ligands and two O atoms from two SiW_{12} anions. The bond distances and angles around the Cu^{II} ions are $1.989(15)$ – $2.011(14) \text{ \AA}$ (Cu–N), $2.484(6)$ – $2.504(11) \text{ \AA}$ (Cu–O), $87.1(6)$ – $178.9(6)^\circ$

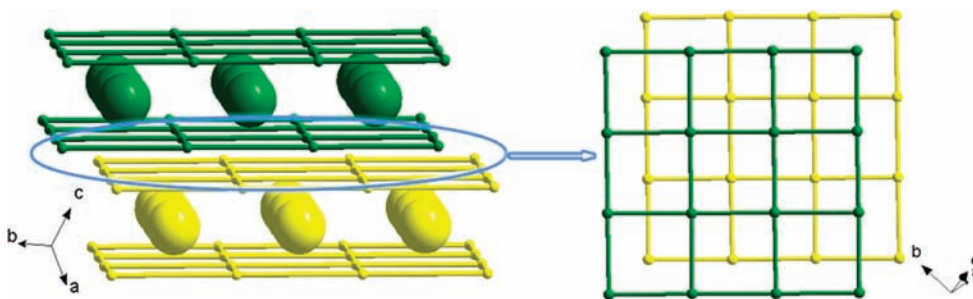


Figure 5. Two adjacent cationic sheets (green and yellow) in different layer units (left) and stagger-peaked (right).

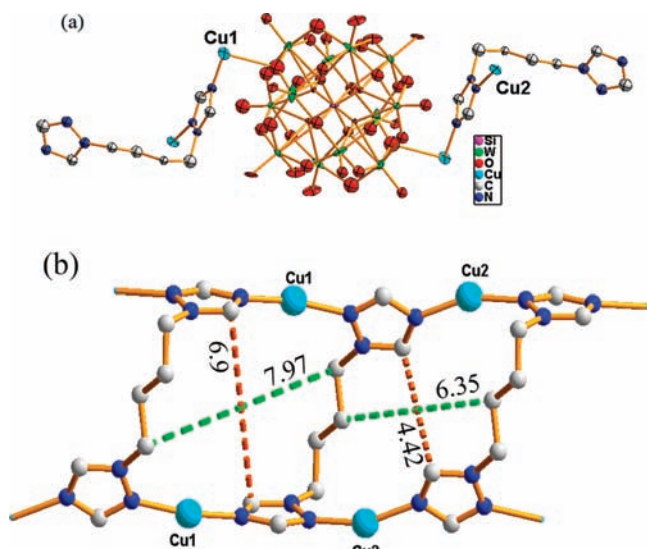


Figure 6. (a) ORTEP drawing of **3** with thermal ellipsoids at 50% probability. The water molecules and H atoms have been omitted for clarity. (b) Two kinds of dinuclear cycles in compound **3**, which connect each other by sharing a side made of a btb ligand.

(N–Cu–N), and $163.5(7)^\circ$ (O–Cu–O), which are similar to those in the six-coordinated Cu^{II} complexes.^{10b} In compound **4**, there exists a hexanuclear cycle that exhibits a stable “chair” conformation, as shown in Figure 8b,c. The dimension of this cycle is ca. $14.82 \times 13.75 \text{ \AA}$, which is big enough to accommodate the SiW₁₂ anion. Therefore, the SiW₁₂ anion is encircled by this hexanuclear cycle through coordination with four of the six Cu^{II} ions, acting as a four-connected linkage. In compound **4**, the btb molecule adopts a single coordination mode, acting as a bidentate ligand to coordinate to two Cu^{II} ions through two apical N atoms, while each Cu^{II} ion is coordinated by four btb ligands. Thus, taking Cu^{II} ions as four-connecting nodes, a 6⁶ (Schläfli symbol) 3D Cu–btb framework is generated (Cu1–Cu1 = 14.13, 11.41, and 8.54 Å). In this open framework, there exist hexagonal channels along the *a* axis. The SiW₁₂ anions acting as four-connected linkages incorporate into the hexagonal channels, as shown in Figure 9.

Stoichiometric Effect of Reactants on the Oxidation State of the Cu Ion and, Furthermore, on Their Coordination Geometries and the Whole Structure. Compounds **1–4** were synthesized under the same conditions, except for using different molar ratios of bis(triazole) ligands to Cu^{II} ions. Therefore, it deserves mention that the stoichiometry of the starting materials acts as a key role in the structural control of the self-assembly process. The Cu

ions change from a reactant Cu^{II} ion to a resultant Cu^I ion under high molar ratios of bis(triazole) to Cu^{II} in the cases of **1** and **3**. The main reason is that the organonitrogen species act as not only ligands but also reductants under hydrothermal conditions. Such a phenomenon has been observed frequently in the hydrothermal reaction system containing N-donor ligands and Cu^{II} ions.^{12b,20}

Both compounds **1** and **2** were obtained in a SiW₁₂–Cu–bte reaction system. However, they had absolutely different frameworks. The difference rested on the molar ratio of the bte ligand to the Cu^{II} ion in the starting materials. Under the 1:3 molar ratio of bte to Cu^{II} for compound **1**, the reactant Cu^{II} ions were reduced to Cu^I ions, which exhibited T-type and “seesaw” geometries. Further, the smart coordination geometries of the Cu^I ions induced the diverse coordination modes of the bte ligands, like the case in **1**. Therefore, the coordination modes of the Cu^I ions and the bte ligands had a synergic influence on the whole framework of compound **1**. However, in compound **2**, the molar ratio (1:15) of bte to Cu^{II} was decreased to one-third of that for compound **1**, and the Cu^{II} ion retained its oxidation state. The Cu^{II} ion in **2** exhibited a single five-coordinated mode, and the bte ligand in **2** also showed a single role, acting as a bidentate bridging ligand. Thus, the simple gridlike Cu^{II}–bte sheet was formed.

Similarly, the stoichiometric effect of btb on the reduction of Cu^{II} was also embodied in the preparations of compounds **3** and **4**. The 1:5 ratio of btb to Cu^{II} in the case of compound **3** resulted in the reduction of Cu^{II} ions to Cu^I ions, and the Cu^I ions also showed diverse coordination modes. However, the btb ligand presented a single tetradentate bridging role with the absence of chelation, perhaps as a result of its long spacer length. The combination of the coordination modes of the Cu^I ions and the bte ligands had a synergic influence on the framework of **3**, namely, a channel-like structure. However, when the ratio of btb to Cu^{II} in the preparation of compound **4** was decreased to 1:14, the Cu^{II} ions retained their oxidation state. The complex of six-coordinated Cu^{II} ions with long btb ligands generated the hexagonal channel framework of **4**, with the SiW₁₂ anions incorporated into the channels.

Template Role of the SiW₁₂ Anion. The four compounds are all based on the SiW₁₂ anion but different Cu^{II/I} centers and ligands with various lengths. The SiW₁₂ anions act as templates to conduce four distinct Cu–bte/btb frameworks. Figure 10 shows detailed views of the Keggin anions surrounded by the Cu–bte/btb moieties to exhibit the interrelations between them in the frameworks of compounds

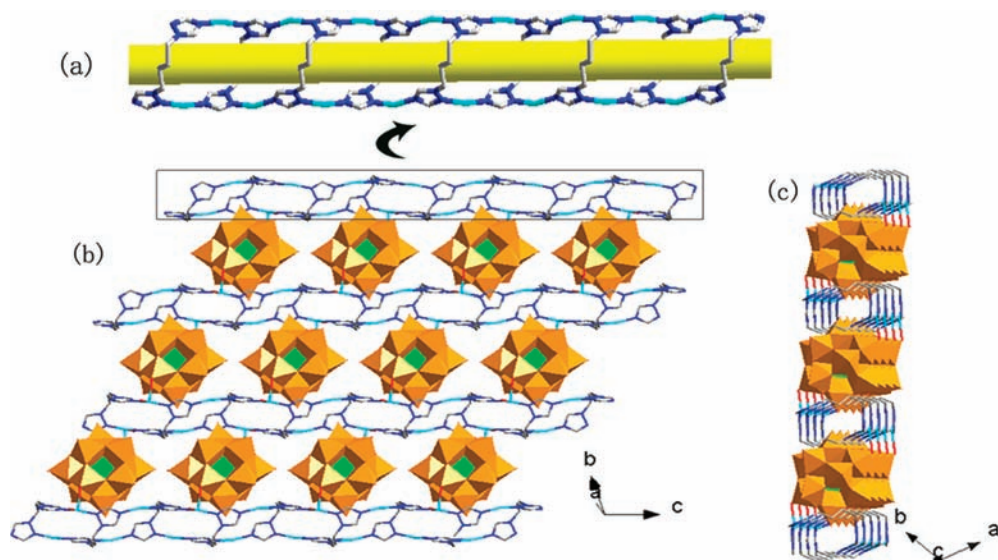


Figure 7. (a) Channel-like chain in compound **3**. Chains and SiW₁₂ anions arranged alternately to construct a 2D layer viewed along (b) the *a* axis and (c) the *c* axis.

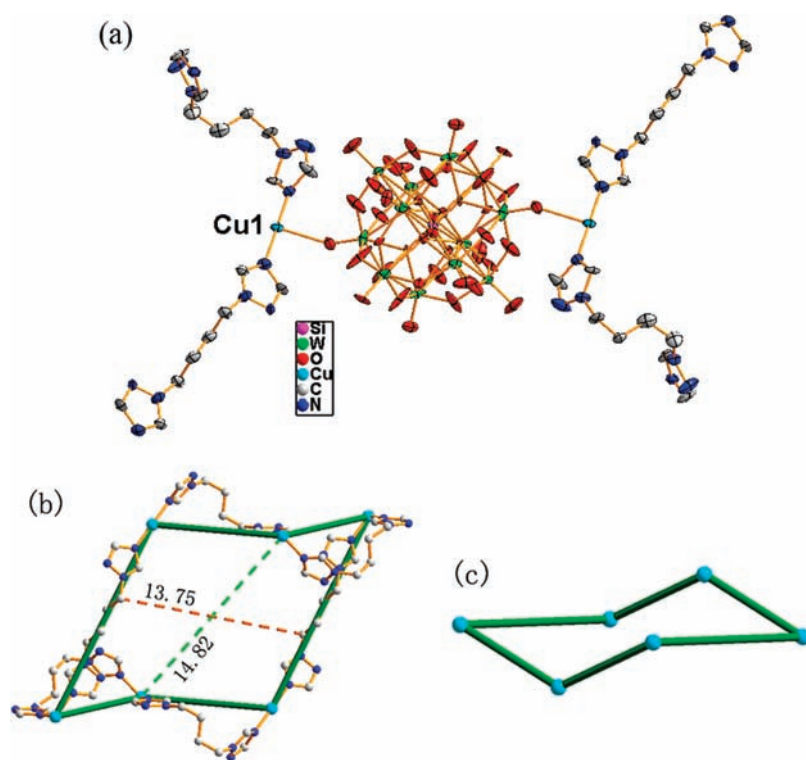


Figure 8. (a) ORTEP drawing of **4** with thermal ellipsoids at 50% probability. The water molecules and H atoms have been omitted for clarity. (b and c) Hexanuclear cycle in compound **4** with the “chair” conformation.

1–4. That is, in compound **1**, there are two types of tetranuclear cycles with dimensions of ca. 11.49×6.12 and 6.15×5.97 Å, respectively. The template anions array up and down only the bigger cycle, owing to their big volumes (ca. 10.38×10.38 Å), while in compound **2**, the anion induces Cu^{II}-btb to form a square tetranuclear grid with a dimension of 11.19×10.71 Å, which is bigger than those in **1**. Thus, two such grids can envelope an anion, just like a “hamburger”. In the case of compound **3**, there exist two kinds of dinuclear cycles with dimensions of ca. 7.97×6.9 and ca. 6.35×4.42 Å, respectively, which are grouped together to form a double-circuit cycle. The big volume of

the template anion only permits a pair of the double-circuit cycles to cover it. In compound **4**, the SiW₁₂ anion induces Cu^{II}-btb to construct a hexanuclear cycle, which encircles the template anion through coordination to four of the six Cu^{II} ions.

FT-IR and XPS Spectra. The IR spectra of compounds **1–4** are shown in Figure S3 in the Supporting Information. In the spectra of **1–4**, characteristic bands at 974, 921, 871, and 790 cm⁻¹ for **1**, 985, 923, 878, and 792 cm⁻¹ for **2**, 967, 919, 878, and 788 cm⁻¹ for **3**, and 979, 923, 871, and 796 cm⁻¹ for **4** are attributed to the $\nu(\text{W}-\text{O}_d)$, $\nu(\text{Si}-\text{O})$, and $\nu(\text{W}-\text{O}_c-\text{W})$ bands, respectively. Bands in the regions

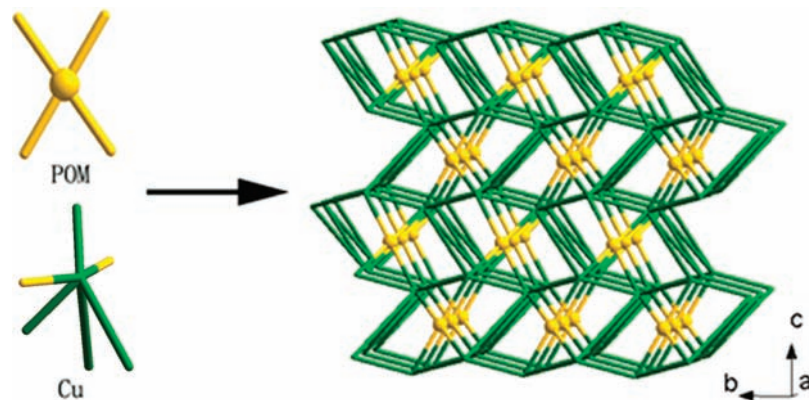


Figure 9. SiW_{12} anions acting as four-connected linkages incorporate into the hexagonal channels of the 3D Cu-btb framework.

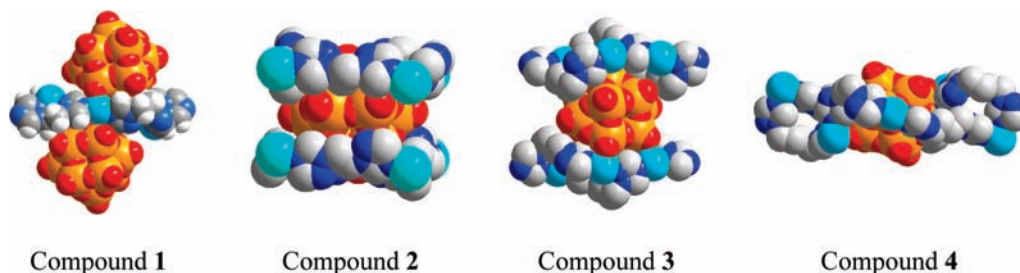


Figure 10. Detailed views of the Keggin anions surrounded by the Cu-bte/btb moieties in compounds 1–4.

of $1686\text{--}1141\text{ cm}^{-1}$ for **1**, $1677\text{--}1128\text{ cm}^{-1}$ region for **2**, $1686\text{--}1143\text{ cm}^{-1}$ for **3**, and $1678\text{--}1132\text{ cm}^{-1}$ for **4** are attributed to the bte and btb ligands.

Figure S4 in the Supporting Information presents the XPS spectra for compounds **1–4**. The XPS spectra show two peaks at 933.9 and 953.8 eV for **1** and at 934.2 and 954.3 eV for **3** attributed to $\text{Cu}^+(2p_{3/2})$ and $\text{Cu}^+(2p_{1/2})$. Two peaks at 935.8 and 955.5 eV for **2** and at 935.9 and 955.7 eV for **4** are attributed to $\text{Cu}^{2+}(2p_{3/2})$ and $\text{Cu}^{2+}(2p_{1/2})$. All of these results further confirm the bond valence sum calculations and the structural analyses.

TGA. The TGA experiments were performed under a N_2 atmosphere with a heating rate of $10\text{ }^\circ\text{C min}^{-1}$ in the temperature range of $40\text{--}800\text{ }^\circ\text{C}$, shown in Figure 11. In the TGA curve for compound **1**, the weight loss of 15.7% (calcd 16.5%) from 300 to $600\text{ }^\circ\text{C}$ corresponds to the loss of bte molecules. The TGA curves of compounds **2–4** show two distinct weight loss steps: The first weight loss steps below $300\text{ }^\circ\text{C}$ correspond to the loss of water molecules. The second weight loss steps in the range of $300\text{--}600\text{ }^\circ\text{C}$ ascribe to the loss of organic molecules, 18.53% (calcd 17.62%) for **2**, 10% (calcd 9.96%) for **3**, and 21.2% (calcd 20.4%) for **4**. Differential thermal analyses (DTA) give the starting decomposition temperatures (DTs) of compounds **1–4**, $335\text{ }^\circ\text{C}$ for **1**, $330\text{ }^\circ\text{C}$ for **2**, $407\text{ }^\circ\text{C}$ for **3**, and $346\text{ }^\circ\text{C}$ for **4**, all higher than $300\text{ }^\circ\text{C}$, whereas transition-metal coordination polymers with similar flexible bis(triazole) ligands, bte and btb, e.g., $[\text{Cu}(\text{bte})_2(\text{dca})_2]_n$, $[\text{Cu}(\text{bte})(\text{NCS})_2]_n$,²⁷ $\{[\text{Mn}(\text{btb})(\text{H}_2\text{O})_4](\text{NO}_3)_2\}_n$,²⁸ and $[\text{Cd}(\text{btb})(\text{H}_2\text{O})_2(\text{NO}_3)_2]_n$,²⁹ all are thermally less stable (DT < $300\text{ }^\circ\text{C}$). Thus,

one can find that these metal-bte/btb coordination polymers based on POMs are more thermally stable than the pure metal–organic frameworks.

Given a detailed comparison of the thermal behaviors for compounds **1–4**, one can find that DT of **3** ($407\text{ }^\circ\text{C}$) is higher than that of **1** ($335\text{ }^\circ\text{C}$) and DT of **4** ($346\text{ }^\circ\text{C}$) is higher than that of **2** ($330\text{ }^\circ\text{C}$). This tendency would be reasonably explained by their structural features. Compounds **1** and **3** have coordination geometries similar to those of the Cu^{I} ions, but the coordination sites of organic ligands and Keggin anions to Cu^{I} in **3** are higher than those in **1**, which may conduce a higher thermal stability of **3**. Similarly, compounds **2** and **4** have a coordination mode identical with that of the organic ligands, and the higher connectivities of the Cu^{II} ions and Keggin anions in **4** than in **2** could make **4** more stable.

Cyclic Voltammetry (CV). Although compounds **1–4** all contain the same Keggin anions, their structures are different. To check whether there exists some structural effect on their redox property, CV measurements are carried out in a $0.5\text{ M H}_2\text{SO}_4 + \text{Na}_2\text{SO}_4$ aqueous solution. Because these compounds are insoluble in water and common organic solvents, the bulk-modified CPE becomes the optimal choice to study their electrochemical properties, which is inexpensive and easy to prepare and handle. The results exhibit almost no structural effect on the redox property, except for some slight potential shifts of the redox peaks (Figure S5 in the Supporting Information). Owing to the similarity of their electrochemical behaviors, only cyclic voltammograms for **1**-CPE at different scan rates in the potential range of $+600$ to -800 mV are described here as examples. There exists one irreversible anodic peak I with the potential of $+346$

(27) Ding, J.-G.; Ge, H.-Y.; Zhang, Y.-M.; Li, B.-L.; Zhang, Y. *J. Mol. Struct.* **2006**, *782*, 143.

(28) Liu, X.-G.; Ge, H.-Y.; Zhang, Y.-M.; Hu, L.; Li, B.-L.; Zhang, Y. *J. Mol. Struct.* **2006**, *796*, 129.

(29) Ding, J.-G.; Liu, X.-G.; Li, B.-L.; Wang, L.-Y.; Zhang, Y. *Inorg. Chem. Commun.* **2008**, *11*, 1079.

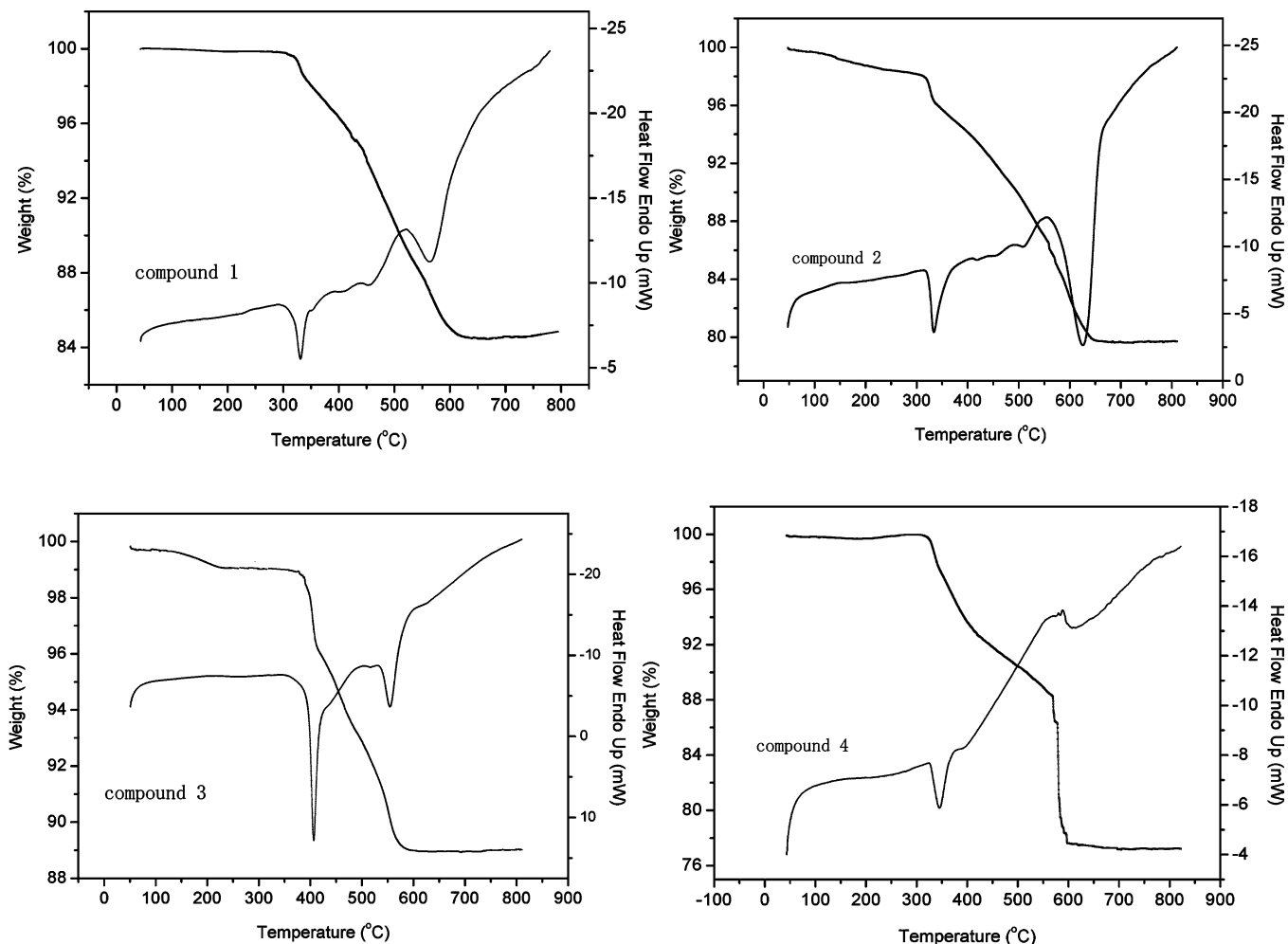


Figure 11. TGA curves for compounds 1–4.

mV assigned to the oxidation of the Cu centers.^{10b,23a} In addition, there exist three reversible redox peaks II–II', III–III', and IV–IV' with half-wave potentials $E_{1/2} = (E_{pa} + E_{pc})/2$ at -328 (II–II'), -534 (III–III'), and -708.5 (IV–IV') mV (scan rate: 100 mV s^{-1}), respectively. Redox peaks II–II' and III–III' correspond to two consecutive one-electron processes of W centers, while IV–IV' corresponds to a two-electron process.³⁰

As compared to the reported SiW_{12} system,³⁰ the slight potential shifts of the three redox peaks in 1-CPE may be related to the combination of copper bis(triazole) complexations. Furthermore, when the scan rates were varied from 100 to 300 mV s^{-1} for 1-CPE, the peak potentials change gradually: the cathodic peak potentials shift toward the negative direction and the corresponding anodic peak potentials toward the positive direction with increasing scan rates.

The results verify that the redox ability of the parent α -Keggin anion can be maintained in the hybrid solids, which promises an application of these kinds of inorganic–organic hybrid materials in electrochemistry.

Conclusion

In this paper, four inorganic–organic hybrid compounds based on Keggin anions have been synthesized under hydrothermal conditions. Through tuning of the molar ratio of the bis(triazole) ligand to Cu^{II} , the reduction of Cu^{II} ions can be realized, and thus the whole structures are influenced. The stoichiometric effects of the reactants on the final frameworks of the title compounds have been confirmed in this work. The synergetic effects of the oxidation states of Cu ions, spacer lengths of the bis(triazole) ligands, and the template role of the SiW_{12} anions lead to diverse structures of the four POM-based compounds in the hydrothermal reaction systems, which enrich the POM family. The TGA results suggest a tendency that the more the connectivities of the Cu ions and the coordination sites of the organic ligands and Keggin anions to Cu ions, the higher the thermal stability of the compounds. However, the diverse structures of the four compounds have no significant influence on their electrochemical properties.

Our attempts show that reasonable syntheses by the hydrothermal technique would be reached to some extent through understanding step by step the influences of various

(30) Sadakane, M.; Steckhan, E. *Chem. Rev.* **1998**, *98*, 219.

factors on the assembly processes, even in a hydrothermal “black box”.

Acknowledgment. This work is financially supported by the National Natural Science Foundation of China (Grant 20671016), the Program for Changjiang Scholars and Innovative Research Team in University, and the Analysis and Testing Foundation of Northeast Normal University.

Supporting Information Available: X-ray crystallographic data in CIF format, tables of selected bond lengths and angles, IR, XPS, and CV data, and structural figures of compounds **1–4**. This material is available free of charge via the Internet at <http://pubs.acs.org>.

IC801338B